

Laser direct growth of graphene on silicon substrate

Dapeng Wei and Xianfan Xu^{a)}

School of Mechanical Engineering and Birck Nanotechnology Center, West Lafayette, Indiana 47907, USA

(Received 4 November 2011; accepted 16 December 2011; published online 10 January 2012)

We demonstrate laser direct growth of few layer graphene on a silicon substrate. In our study, a continuous wave laser beam was focused on a poly(methyl methacrylate) (PMMA)-coated silicon wafer to evaporate PMMA and melt the silicon wafer. Carbon atoms, decomposed from PMMA, were absorbed by the molten silicon surface, and then separated from silicon in the cooling process to form few-layer graphene. This Si-catalyzed method will provide a new approach and platform for applications of graphene. © 2012 American Institute of Physics. [doi:10.1063/1.3675636]

Owing to the unique structural and electrical properties, graphene, a two-dimensional atomic-thick crystal with carbon atoms packed in a honeycomb lattice, is regarded as one of the most important materials for future high-performance devices.^{1–3} As the first step for these applications, synthesis of graphene has been the focus of research in recent years.^{2,4} Until now, CVD (chemical vapor deposition) has been a main route to obtain large-scale high-quality graphene, though other techniques have also been developed to produce single or few-layer graphene, such as thermal decomposition of SiC,⁵ arc charge,⁶ and carbon nanotube (CNT) unzipping.⁷ In a CVD process, Cu, Ni, or other metals act as catalyst through surface precipitation of carbon.^{8–10} In addition to vapor phase carbon sources such as CH₄ and C₂H₂, solid carbon source has also been used. Sun *et al.* produced graphene on Cu and Ni film using poly(methyl methacrylate) (PMMA).¹¹ Due to the existence of the metal films, the graphene films need be transferred to other substrate using polydimethylsiloxane (PDMS) (Ref. 12) or PMMA (Ref. 13). Silicon wafer is the most important single-crystal substrate used for semiconductor devices and integrated circuits. Suenitsu *et al.* produced epitaxial graphene on Si substrate.¹⁴ In their approach, a SiC film of about 100 nm-thick was deposited on the Si wafer before growth, so graphene was grown on the SiC surface. Direct growth of graphene on bare Si substrate without any other material is very attractive. Graphene films can form a Schottky junction with Si, which can produce a built-in electric field and realize electron-hole separation, and has been used to fabricate solar cells.¹⁵

In this work, we demonstrate direct synthesis of few-layer graphene on silicon. A PMMA film, coated on a Si substrate, was used as carbon source. Thermal energy is provided by laser irradiation. Laser synthesis of graphene on SiC has been reported.¹⁶ In our approach, laser irradiation evaporates and decomposes the PMMA film and melts the surface of silicon. The carbon atoms are then absorbed and dissolved in melted silicon. In the cooling process, the dissolved carbon is extracted from the melted silicon to form few-layer graphene.

A 1 cm × 2 cm p-type (111)-oriented Si wafer was used as the substrate to grow graphene. The silicon wafer was cleaned and the native oxide layer was removed in buffer

hydrofluoric acid (HF) solution to form H-terminated silicon surface. A PMMA (nano 950 K PMMA 4% in Anisole) layer was coated on the Si surface by spin coating. The PMMA-coated Si substrate was covered by a quartz wafer of the same size, and then the quartz and silicon wafers were fixed on a sample stage using two spring clamps. The purpose of using the quartz wafer is to maintain a high enough concentration of carbon after PMMA is evaporated and dissociated by laser irradiation. The growth was conducted in a vacuum chamber, which was pumped and purged using high-purity N₂ gas, and then maintained at a pressure below 0.1 Torr. A continuous wave (CW) Nd:YAG laser with a wavelength of 532 nm was focused on the Si surface using a lens of 150 mm focal length. The diameter of the laser spot on the sample surface is about 20 μm. In our system, a laser power of 3.1 W can melt the surface of the Si wafer.

Figure 1(a) is an SEM (scanning electron microscopy, Hitachi S-4800) image of the laser-irradiated area, showing that irradiation of the laser beam generates a circular area with a visible boundary. The diameter of the laser-irradiated area is about 20 μm, similar to the laser spot size. The laser power used is 3.1 W, and the heating time is 5 min. The higher magnification SEM image in Fig. 1(b) shows that due to melting of silicon, the surface is not even at a scale of micrometer. Raman spectroscopy is a powerful tool for characterizing graphene, which can provide rich structural information. In general, there are three major Raman peaks around 1350 cm⁻¹ (D band), 1580 cm⁻¹ (G band), and 2700 cm⁻¹ (2D band). The D band is due to first-order scattering by zone-boundary phonons caused by disorder or defect in the sp² C, such as point defects, subdomain boundaries, and edges.^{17–19} The G band is associated with the doubly degenerate zone center E_{2g} mode.²⁰ The ratio between the Raman intensities of D and G bands, I(D)/I(G), is an important factor for evaluating the amount of structural defects and the domain size of graphene.^{17,18} The 2D band is associated with second-order scattering by zone-boundary phonons.²¹ 2D Raman band shape, position, full width at half-maximum (FWHM), and I(G)/I(2D) ratio are finger prints to identify the number of layers of graphene.^{8,11,21,22} In our study, Raman measurements were carried out with laser excitation at 532 nm (Horiba Jobin Yvon XploRA). A 100 × objective lens was used, and the laser spot size was ~0.6 μm. Each spectrum was an average of 3 acquisitions (10 s of accumulation time per acquisition). Figures

^{a)} Author to whom correspondence should be addressed. Electronic mail: xxu@purdue.edu.

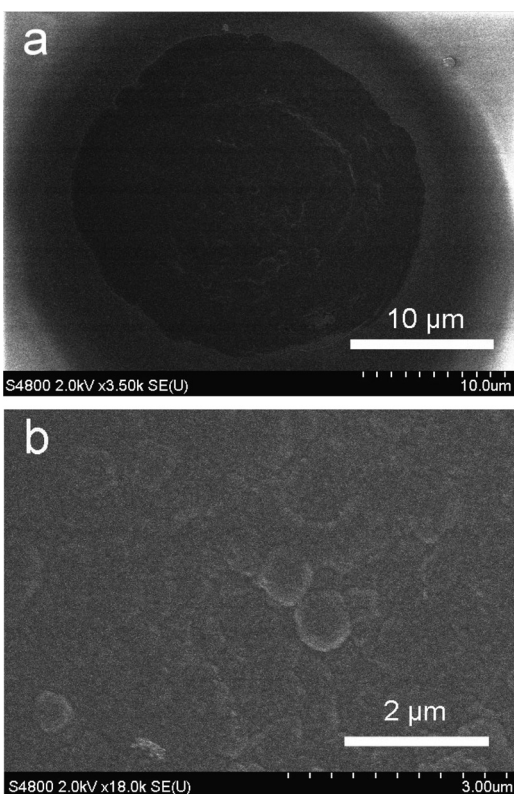


FIG. 1. Growth of graphene using a PMMA-coated Si covered by a quartz wafer, with a laser power of 3.1 W for 5 min. (a) SEM image of laser-processed Si surface; (b) a magnified SEM image of the center of the laser-irradiated area.

2(a)–2(c) are typical Raman mapping of the D, G, and 2D bands. The brightness is proportional to the height of Raman peak. Figure 2(a) shows that the higher D peak appears on the edge of the graphene, the same as previous Raman studies of graphene edges.^{19,23} Meanwhile, the graphene growth area has the same shape and size as the laser-irradiated area in Fig. 1, which confirms that the growth of graphene only happens in the laser-melted Si surface. Figure 2(d) shows typical Raman spectra from the central area. A weak D peak at 1348 cm^{-1} and a strong G peak at 1590 cm^{-1} are apparent. The $I(D)/I(G)$ ratio is about 0.076, which indicates that the graphene has good quality with a few defects. In general, the 2D band position at 2680 cm^{-1} (Ref. 8) and FWHM of about 30 cm^{-1} (Refs. 11 and 22) are related to monolayer graphene. In our case, the 2D band is located at 2685 cm^{-1} , and its FWHM is about 38 cm^{-1} . Up-shifted and boarder 2D band compared with monolayer graphene suggest the as-grown graphene has two or more layers. In addition, the Raman spectra has an $I(G)/I(2D)$ ratio of 1.01, indicating most of the products are bi- or tri-layer graphene.^{8,11,22,24}

As mentioned previously, a quartz wafer was fixed on top of PMMA-coated silicon for maintaining a high enough concentration of carbon from laser-dissociated PMMA. For comparison, experiments were also preformed without using the quartz wafer. The resulting Raman signals were much weaker and discontinuous in the laser heated area. On the other hand, when the quartz wafer was used, there would be a small gap between the quartz wafer and the silicon substrate during laser heating due to localized thermal expansion in the laser heated area. The gap size is estimated to be of

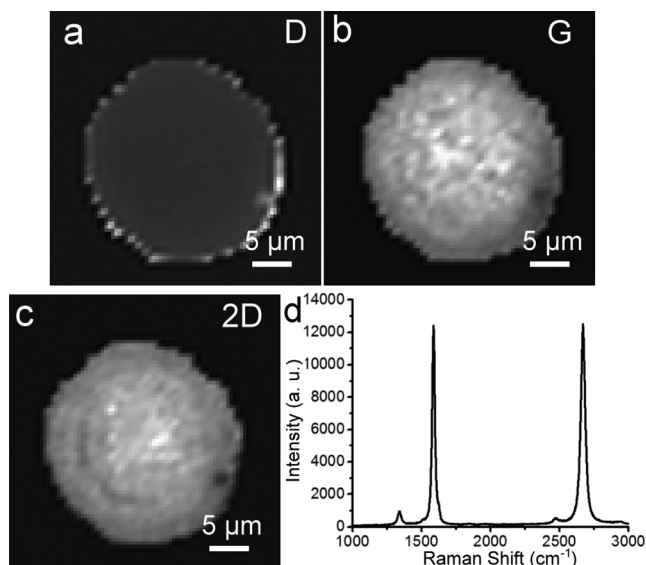


FIG. 2. (a)–(c) Raman maps of the D (1300 to 1400 cm^{-1}), G (1560 to 1620 cm^{-1}), and 2D (2660 to 2700 cm^{-1}) bands, respectively. The wavelength of the Raman excitation laser is 532 nm . (d) Typical Raman spectra recorded from the central area in (a)–(c).

the order of micrometers using thermal expansion coefficients of the wafers and the estimated temperature rise. This narrow gap provided a leakage path for laser-dissociated gases.

For growth of graphene on metal, two main growth mechanisms were proposed. On Ni, graphene was produced via carbon dissolution and precipitation.⁹ On Cu, the growth can be explained by surface-catalyzed process, which involves carbon nucleation on the Cu surface, and the growth of graphene with the addition of carbon to the edges.²³ However, both of these growth mechanisms cannot explain the graphene growth on Si. Cu or Ni maintains solid in the graphene growth process. We found that if the laser power was below the melting point of silicon, there was no graphene grown on the silicon surface.

Figures 3(a)–3(f) are optical images of the laser-irradiated areas with different illumination times. In less than 1 s, PMMA in the center of the laser-irradiated area was removed, but the bare silicon surface had no visible change. During laser heating, the edge of PMMA film was melted and evaporated continuously, exposing a larger bare silicon surface. Outside this bare silicon surface, PMMA is intact. At 3 min, a small dark spot can be seen at the center of the laser-illuminated area, indicating that the temperature of the silicon surface reached the melting point. From 3 to 15 min, the diameter of the dark spot increased continuously. At 15 min, the surface tension as well as evaporation forced liquid silicon to form a crater-shaped surface topography.^{25,26} Figure 3(g) is the Raman spectra recorded at the center of laser-irradiated areas. Before or at the beginning of the silicon melting process, no Raman peaks could be observed. As melting continues for several minutes, Raman signals of graphene appear. According to the C-Si binary phase diagram, the solid solubility of C in Si at 1200 to $1400\text{ }^{\circ}\text{C}$ is only $\sim 10^{-4}$ to 10^{-3} at. %, while the solubility of C in liquid Si at the eutectic point ($1404\text{ }^{\circ}\text{C}$) is about 0.75 at. %. Therefore, there is not enough carbon absorbed by solid Si for the

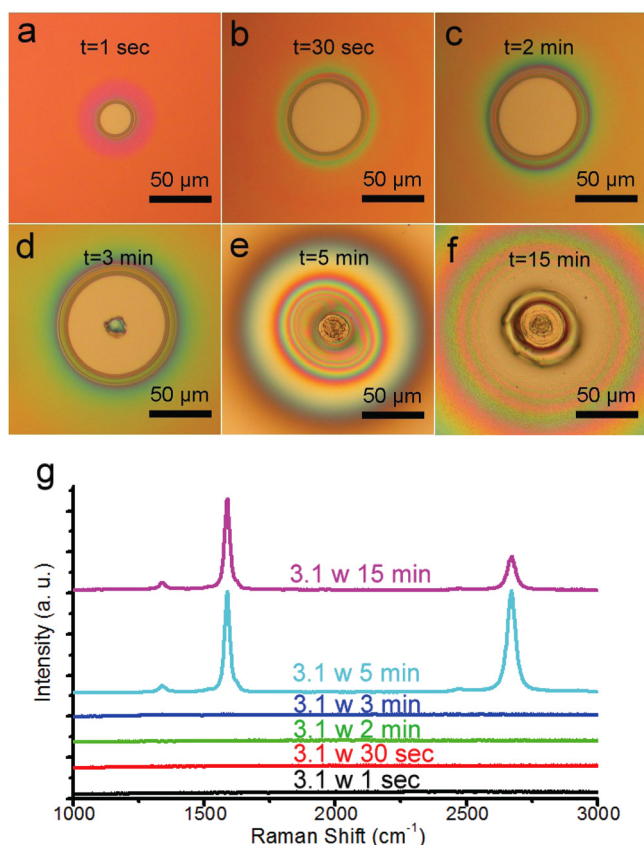


FIG. 3. (Color online) (a)–(f) Optical micrographs of laser-irradiated areas. The laser power is 3.1 W and the illumination time is 1 s, 30 s, 2 min, 3 min, 5 min, and 15 min, respectively. (g) The corresponding Raman spectra recorded from the center of the laser-irradiated area in (a)–(f).

formation of graphene. When illuminated for 5 min, the Raman spectrum is similar to that in Fig. 2, indicating formation of 2–3 layer graphene. When illuminated for 15 min, the $I(G)/I(2D)$ ratio is 2.67, which signifies the as-grown graphene has no less than 4 layers.²⁴

Based on the above discussions, the growth of graphene on Si is a liquid-Si-catalyzed process. PMMA was decomposed on the surface of molten silicon. The diffusion of carbon atoms into molten silicon took several minutes in order for silicon to absorb enough carbon atoms. In the cooling process, the decrease of the solubility of C drove the C-Si separation, and the precipitated carbon atoms were coalesced and nucleated to form a graphene film.

In summary, we synthesized few-layer graphene on silicon without any metal catalyst using laser-heated CVD. It was found that the silicon surface was melted under laser irradiation, and liquid Si acted as a catalyst to absorb, dissolve, and finally extract carbon atoms to form graphene. The amount of absorbed carbon atoms can be controlled by the laser illumination time, which determines the number of

graphene layers. The method can potentially be scaled up for wafer scale manufacturing using the “flash and step” method similar to that used in photolithography.

The authors are grateful to Professor Yong P. Chen, Dr. Dacheng Wei, Dr. Xin Xu, and James Mitchell for helps in the experiments and discussions. We acknowledge the support of the Defense Advanced Research Projects Agency (Grant No. N66001-08-1-2037) and the National Science Foundation (Grant Nos. DMI-0707817 and CMMI-1120577).

- ¹K. S. Novoselov, A. K. Geim, S. V. Morozov, D. Jiang, M. I. Katsnelson, I. V. Grigorieva, S. V. Dubonos, and A. A. Firsov, *Nature (London)* **438**, 197 (2005).
- ²D. C. Wei and Y. Q. Liu, *Adv. Mater.* **22**, 3225 (2010).
- ³M. J. Allen, V. C. Tung, and R. B. Kaner, *Chem. Rev.* **110**, 132 (2010).
- ⁴W. Choi, I. Lahiri, R. Seelaboyina, and Y. S. Kang, *Crit. Rev. Solid State Mater. Sci.* **35**, 52 (2010).
- ⁵M. Sprinkle, M. Ruan, Y. Hu, J. Hankinson, M. Rubio-Roy, B. Zhang, X. Wu, C. Berger, and W. A. de Heer, *Nature Nanotechnol.* **5**, 727 (2010).
- ⁶L. S. Panchokarla, K. S. Subrahmanyam, S. K. Saha, A. Govindaraj, H. R. Krishnamurthy, and U. V. Waghmare, *Adv. Mater.* **21**, 4726 (2009).
- ⁷L. Y. Jiao, L. Zhang, X. R. Wang, G. Diankov, and H. J. Dai, *Nature (London)* **458**, 878 (2009).
- ⁸X. Li, W. Cai, J. An, S. Kim, J. Nah, D. Yang, R. Piner, A. Velamakanni, I. Jung, E. Tutuc *et al.*, *Science* **324**, 1312 (2009).
- ⁹Q. Yu, J. Lian, S. Siriponglert, H. Li, Y. P. Chen, and S. Pei, *Appl. Phys. Lett.* **93**, 113103 (2008).
- ¹⁰D. Eom, D. Prezzi, K. T. Rim, H. Zhou, M. Lefenfeld, S. X. Xiao, C. Nuckolls, M. S. Hybertsen, T. F. Heinz, and G. W. Flynn, *Nano Lett.* **9**, 2844 (2009).
- ¹¹Z. Z. Sun, Z. Yan, J. Yao, E. Beitler, Y. Zhu, and J. M. Tour, *Nature (London)* **468**, 549 (2010).
- ¹²K. S. Kim, Y. Zhao, H. Jang, S. Y. Lee, J. M. Kim, K. S. Kim, J. H. Ahn, P. Kim, J. Y. Choi, and B. H. Hong, *Nature (London)* **457**, 706 (2009).
- ¹³A. Reina, X. T. Jia, J. Ho, D. Nezich, H. Son, V. Bulovic, M. S. Dresselhaus, and J. Kong, *Nano Lett.* **9**, 30 (2009).
- ¹⁴M. Suemitsu and H. Fukidome, *J. Phys. D: Appl. Phys.* **43**, 374012 (2010).
- ¹⁵X. M. Li, H. W. Zhu, K. L. Wang, A. Y. Cao, J. Q. Wei, C. Y. Li, Y. Jia, Z. Li, X. Li, and D. H. Wu, *Adv. Mater.* **22**, 2743 (2010).
- ¹⁶S. Lee, M. F. Toney, W. Ko, J. C. Randel, H. J. Jung, K. Munakata, J. Lu, T. H. Geballe, M. R. Beasley, R. Sinclair *et al.*, *ACS Nano* **4**, 7524 (2010).
- ¹⁷M. A. Pimenta, G. Dresselhaus, M. S. Dresselhaus, L. G. Cancado, A. Jorio, and R. Saito, *Phys. Chem. Chem. Phys.* **9**, 1276 (2007).
- ¹⁸A. C. Ferrari, *Solid State Commun.* **143**, 47 (2007).
- ¹⁹C. Casiraghi, A. Hartschuh, H. Qian, S. Piscanec, C. Georgi, A. Fasoli, K. S. Novoselov, D. M. Basko, and A. C. Ferrari, *Nano Lett.* **9**, 1433 (2009).
- ²⁰F. Tuinstra and J. Koenig, *J. Chem. Phys.* **53**, 1126 (1970).
- ²¹A. C. Ferrari, J. C. Meyer, V. Scardaci, C. Casiraghi, M. Lazzeri, F. Mauri, S. Piscanec, D. Jiang, K. S. Novoselov, S. Roth *et al.*, *Phys. Rev. Lett.* **97**, 187401 (2006).
- ²²A. Reina, X. T. Jia, J. Ho, D. Nezich, H. Son, V. Bulovic, M. S. Dresselhaus, and J. Kong, *Nano Lett.* **9**, 30 (2009).
- ²³Q. Yu, L. A. Jauregui, W. Wu, R. Colby, J. Tian, Z. Su, H. Cao, Z. Liu, D. Pandey, D. Wei *et al.*, *Nature Mater.* **10**, 443 (2011).
- ²⁴H. Cao, Q. Yu, R. Colby, D. Pandey, C. S. Park, J. Lian, D. Zemlyanov, I. Childres, V. Drachev, E. A. Stach *et al.*, *J. Appl. Phys.* **107**, 044310 (2010).
- ²⁵D. A. Willis and X. Xu, *J. Heat Transfer* **122**, 763 (2000).
- ²⁶D. A. Willis, X. Xu, C. C. Poon, and A. T. Tam, *Opt. Eng.* **37**, 1033 (1997).